# Optical rotatory power of different phases of an antiferroelectric liquid crystal and implications for models of structure

N. M. Shtykov,[1,*] J. K. Vij,[1,†] and H. T. Nguyen[2]
[1]*Department of Electronic and Electrical Engineering, Trinity College, University of Dublin, Dublin 2, Ireland*
[2]*Centre de Recherche Paul Pascal/CNRS, Université de Bordeaux I, Avenue A. Schweitzer, F-33600 Pessac, France*
(Received 20 June 2000; revised manuscript received 26 October 2000; published 25 April 2001)

The antiferroelectric liquid crystal (AFLC) under investigation possesses different helical smectic phases. The various phases have been identified through a texture under cross-polarizers with a homeotropic alignment of the AFLC. Measurements of the optical rotatory power (ORP) of these phases have elucidated the ability of this method for finding phase transitions between several phases and for investigating the helical structure of the antiferroelectric phases. The optical rotatory power as a function of temperature at a fixed wavelength of light was measured for different phases of the investigated AFLC material. The values of the pitch for some of the phases have been calculated from the ORP data. The results of the ORP rule out the simple ''clock'' model or a clock model with a long pitch superimposed on to it. The results can be explained only in terms of biaxial models, either Ising-type models or a highly distorted ''clock'' model. It is also found that in the Sm$C_A^*$ phase the sense of the helix in the investigated material is left handed, and is opposite to that observed in the Sm$C^*$ phase. The reversal of the helix from left to right handed occurs during the phase transition from the Sm$C_{FI1}^*$(Sm$C_\gamma^*$) to Sm$C_{FI2}^*$(AF) phase. This fact also allows for Sm$C_A^*$ and AF phases to be distinguished from each other.

DOI: 10.1103/PhysRevE.63.051708 PACS number(s): 42.70.Df, 61.30.−v, 64.70.Md

## I. INTRODUCTION

Antiferroelectric liquid crystals (AFLC's) exhibit several chiral phases between paraelectric smectic $A$(Sm$A^*$) and antiferroelectric smectic $C_A$(Sm$C_A^*$). These phases were tentatively designated as Sm$C_\alpha^*$, Sm$C_\beta^*$, and Sm$C_\gamma^*$ in order of decreasing temperature [1]. Among these phases Sm$C_\alpha^*$ seems to be a more complicated phase than the other phases. A number of additional ferrielectric and antiferroelectric phases were discovered. The Sm$C_\beta^*$ phase is usually considered to be the same as the ferroelectric chiral smectic $C$(Sm$C^*$), but in optically pure samples some peculiarities can be observed [2]. An x-ray resonant technique employed on a thiobenzoate liquid-crystal compound recently showed [3,4] the existence of four phases with different superlattice periodicities. These phases are Sm$C_A^*$, Sm$C_{FI1}^*$, and Sm$C_{FI2}^*$ with two-, three-, and four-layer superlattices, respectively, and Sm$C_\alpha^*$ with a periodicity incommensurate with the layer spacing. In the Sm$C_\alpha^*$ phase an incommensurate periodicity was shown to roughly lie in between eight and five layers with decreasing temperature.

Several different theoretical approaches were advanced for explaining a variety of ferroelectric phases, and these postulates were based mostly at the expanded Landau model [5] or on the one-dimensional Ising model [6] and the axial next-nearest-neighbor Ising model [7,8]. Recently, the short pitch mode model [9] was presented, which describes antiferroelectric and ferroelectric phases as structures with certain ''families'' of modulation modes.

Light transmission through a homeotropic liquid-crystal (LC) cell placed between two crossed polarizers was measured, and the optical rotatory power was calculated from these results. The transmission as a function of temperature was measured in different smectic phases of the AFLC material at several wavelengths of light. Dielectric and polarizing microscopies were also carried out to complement the optical transmission results. The helical pitch of the structures in different phases of AFLC material was obtained from the optical rotatory power. The results of pitch values for the various phases are given.

## II. EXPERIMENT

The AFLC material used in our experiments is the $n=11$ member (with acronym 11OTBBB1M7) of the homologous series, whose molecular structure is given as

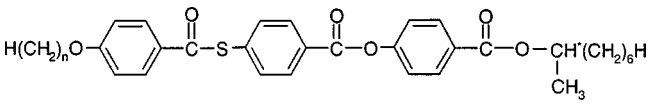


The following phase transition sequence for this material has been found for the bulk sample by the DSC method: crystal (95.5 °C) Sm$C_A^*$ (101 °C) Sm$C_{FI1}^*$ (104.5 °C) Sm$C_{FI2}^*$ (111 °C) Sm$C^*$ (127 °C) Sm$C_\alpha^*$ (128 °C) Sm$A^*$ (149 °C) isotropic. This phase sequence corresponds to that given by Nguyen *et al.* [10]. The tenth member (10OTBBB1M7) of the same homologous series was recently investigated using resonant x-ray diffraction [3,4].

A cell of 15-$\mu$m sample thickness, used for dielectric and optic measurements, consisted of two glass plates with a ITO (indium tin oxide) layers as electrodes and Mylar thin-film stripes as spacers. Homeotropic orientant films of a carboxylato chromium complexes (chromolane) purchased from

*Permanent address: Institute of Crystallography, Russian Academy of Sciences, 117333, Moscow, Leninsky prosp. 59, Russia.
†Email address: jvij@tcd.ie

 

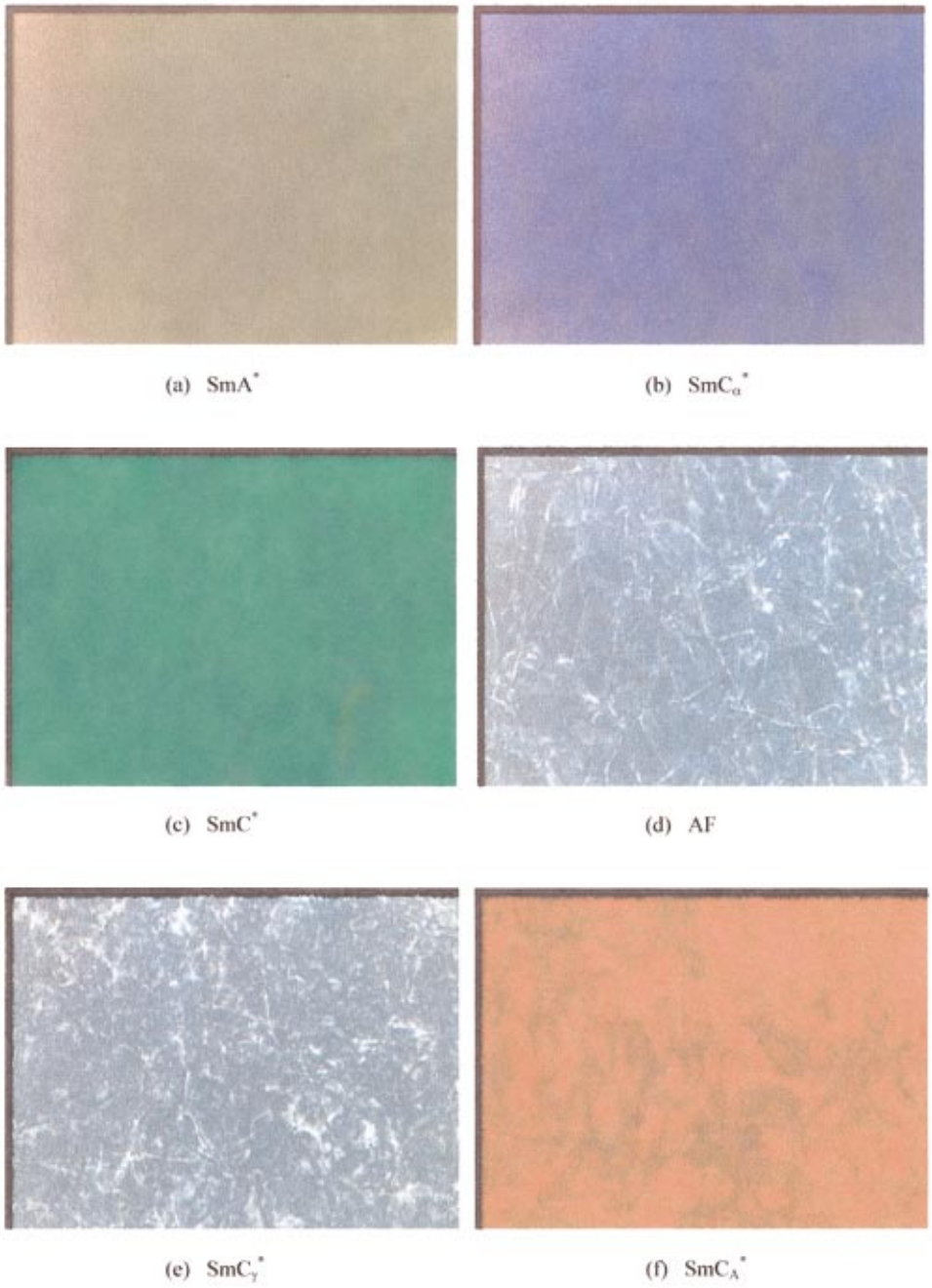


FIG. 1. (Color) Sequence of microscopic textures obtained upon cooling a homeotropic sample of 11OTBBB1M7; (a) Sm-$A$* (133 °C). (b) Sm-$C^*_\alpha$ (129 °C) color is changed to blue. (c) Sm-$C$* (118 °C); color is changed to green. (d) Sm-$C^*_{FI2}$ (108 °C) and (e) Sm-$C^*_{\mathrm{FI1}}$ (101 °C) are gray. (f) Sm-$C^*_A$ (98 °C); the color is altered to red.

AURAT Joint Co. Moscow, Russia, were coated on the ITO electrodes, cured for a duration of 0.5 h at a temperature of 120 °C and then used without rubbing. The cell was heated and filled with the antiferroelectric compound in the isotropic phase, and cooled slowly to the Sm$A$* phase. The textures of the different smectic phases were observed with a charge-coupled device camera, fitted to a polarizing microscope, and captured by a corresponding video grabber in a computer. Dielectric measurements at a frequency of 1 kHz were made using the impedance analyzer HP-4192A. The temperature measurements were carried out during continuous cooling at a rate of 0.1 °C/min.

The optical rotatory power (ORP) was calculated from the ratio of the light transmitted through the homeotropic liquid crystal cell when polarizers were crossed to when these were parallel to each other. For the case of pure optical rotation, when the light transmitted through the cell remains linearly polarized, the ratio of these transmissions $R_T$ is given by a simple expression $R_T(\psi)=\tan^2\psi$. Here $\psi$ is a rotation angle of the light transmitted through the cell with respect to the polarizer direction. The ORP ($\Psi$) is defined as the optical rotation per unit length $\psi/d$, where $d$ is the cell thickness, and can be calculated from the transmission with the use of expression

$$\Psi=\frac{\tan^{-1}\sqrt{R_T(\psi)}}{d}. \tag{1}$$

This method gives only the absolute value of the ORP. The sign of the ORP in several smectic phases was determined by

rotating the analyzer until the minimum of the transmission was achieved. The clockwise turn of an analyzer (with respect to the position where it is crossed with a polarizer) is considered to be positive, and the anticlockwise turn to be negative.

### III. RESULTS AND DISCUSSION

According to the optical and dielectric results for a thin homeotropic cell on cooling 11OTBBB1M7, the following phase transition sequence is observed: crystal (84 °C) Sm$C_A^*$ (100 °C) Sm$C_{FI1}^*$ (103.2 °C) Sm$C_{FI2}^*$ (110.6 °C) Sm$C^*$ (127.8 °C) Sm$C_\alpha^*$ (131.1 °C) Sm$A^*$ (151.2 °C) isotropic. When the sample is heated, the melting temperature is found to be 97.5 °C. One can see a small difference in the phase transition temperatures between our results and those already given [10]. The difference in the transition temperatures is due to the influence of the boundary conditions on the phase transition temperatures for a thin sample. Most of the observed phases have approximately the same temperature range as the bulk sample, except the Sm$C_\alpha^*$ phase, the temperature range of which increased by 2 °C as a consequence of the decrease in the temperature for the Sm$A^*$ phase.

Figure 1 shows the textures in black and white at crossed polarizers that have been obtained for smectic phases on cooling the homeotropic cell of a 11OTBBB1M7 compound. A homeotropic alignment in the Sm$A^*$ phase [Fig. 1(a)] has a very uniform texture. The Sm$C_\alpha^*$ phase [Fig. 1(b)] looks like the Sm$A^*$ phase, except that, its color was altered to blue. But in Sm$C^*$, Sm$C_{FI2}^*$, Sm$C_{FI1}^*$, and Sm$C_A^*$ phases [Figs. 1(c)–(b)], disinclination lines appear. Sm$C^*$ was seen as green, and Sm$C_{FI2}^*$ and Sm$C_{FI1}^*$ were seen as gray. The structure inhomogeneities are noted especially in the Sm$C_{FI1}^*$ phase [Fig. 1(e)]. The reason that Fig. 1(b) is a Sm$C_\alpha^*$ phase but not Sm$C^*$ phase is the absence of disinclination lines. The bright uniform colors of the Sm$C^*$ [Fig. 1(c)], seen as green, and the Sm$C_A^*$ phase [Fig. 1(f)] seen as red, mean that helical pitches of these phases are comparable to the wavelength of visible light. Despite the presence of disinclination lines, the homeotropic alignment of a sample is sufficiently uniform. The dielectric results (Fig. 2) also confirm this assumption. There are no contributions of the Goldstone mode to the dielectric permittivity $\varepsilon'$ and the dielectric loss $\varepsilon''$.

The temperature dependencies of the light transmitted through the cell, placed between the crossed polarizers, are shown in Fig. 3 for different wavelengths. For green light ($\lambda = 523$ nm), one sees a stepwise increase of the transmission in the low temperature region of the Sm$C^*$ phase. This steplike behavior is more pronounced close to the phase transition to the antiferroelectric Sm$C_{FI2}^*$ phase. The steps are less pronounced for the blue-green light ($\lambda = 494$ nm) and were not observed for yellow and red light [Fig. 3(b)]. The nature of this steplike behavior is not clear now. We should note that the temperature dependencies of the transmission for wavelengths of yellow and red light differ from those for blue and green light.

The ORP calculated from light transmission using Eq. (1) and shown in Fig. 4 demonstrates a characteristic change in each phase. The value of the ORP in the Sm$C_\alpha^*$ phase is very low. This confirms the predictions of the clock model [11], according to which the Sm$C_\alpha^*$ phase is characterized by a short-pitch helical structure. But there is a discrepancy between values of this pitch measured by different methods. Resonant x-ray measurements [3,4] give a decrease in the pitch from eight- to five-layer periodicity with decreasing temperature. An ellipsometric study [12] showed that the helical pitch increases from 20- to 40-layer periodicity when the temperature decreases. It is possible that this difference in the temperature dependence and pitch magnitude is related to different phase sequences in these two compounds. The sign of the ORP in the Sm$C^*$ and Sm$C_{FI2}^*$ phases is the same for short wavelengths, but is the opposite for Sm$C_{FI1}^*$ and Sm$C_A^*$ phases. This means that the handedness of the chiral structure is changed during a transition from the Sm$C_{FI2}^*$ phase to the Sm$C_{FI1}^*$ phase. The sign of the ORP in the Sm$C^*$ phase is the same for short wavelengths (494 and 523 nm) but is the opposite for long wavelengths (587 and 619 nm). According to Eq. (2) this means that the wavelength of the selective reflection is located between wavelengths of 523 and 587 nm. This fact is confirmed by visual observation.

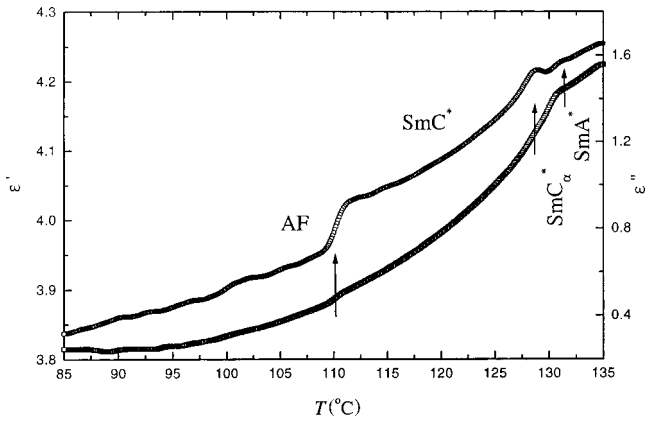


FIG. 2. Dependencies on temperature of the dielectric permittivity $\varepsilon'$ and loss $\varepsilon''$ of a homeotropic sample at a frequency 1 kHz in several smectic phases.

The ORP in cholesteric LC is given as [13]

$$\Psi = \frac{2\pi}{8P}\left(\frac{n_e^2 - n_o^2}{n_e^2 + n_o^2}\right)^2 \frac{1}{\lambda'^2(1-\lambda'^2)}, \tag{2}$$

$$n = \left(\frac{n_e^2 + n_o^2}{2}\right)^{1/2}, \tag{3}$$

$$\lambda' = \frac{\lambda}{nP}, \tag{4}$$

where $P$ is the helical pitch, $\lambda$ is the wavelength in vacuo, and $n_e$ and $n_o$ are the refractive indices parallel and perpendicular to the director. This expression can be extended to the tilted smectic phases using the relations [14]

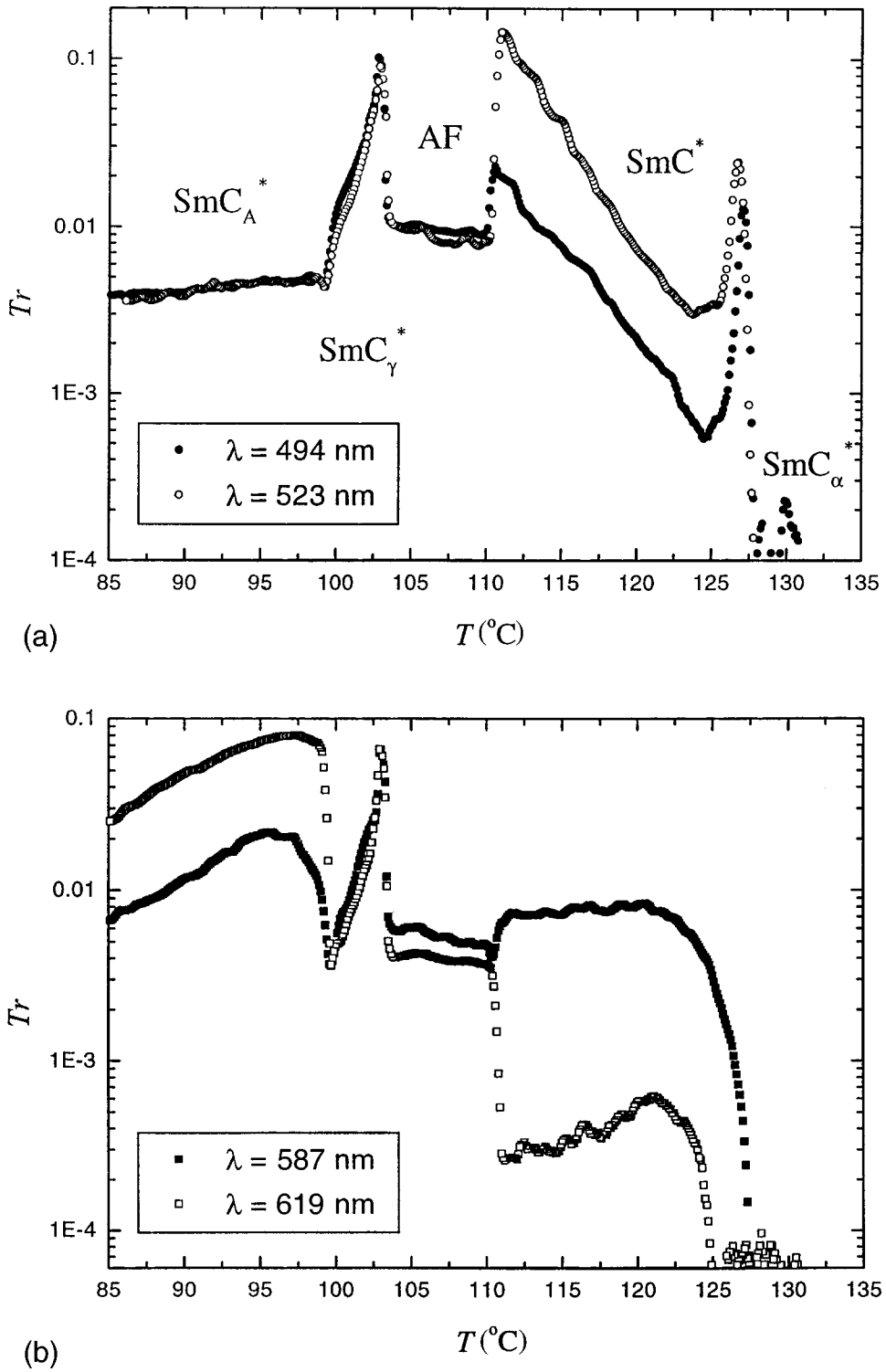


FIG. 3. Temperature dependencies of the light transmission through a homeotropic cell placed between crossed polarizers. (a) For blue-green (494 nm) and green (523 nm) light. (b) For yellow (587 nm) and red (619 nm) light.

$$n_e^2 = \frac{\varepsilon_{10}\varepsilon_{30}}{\varepsilon_{10}\cos^2\theta + \varepsilon_{30}\sin^2\theta}, \tag{5}$$

$$n_o = \sqrt{\varepsilon_{20}}, \tag{6}$$

where $\varepsilon_{10}$, $\varepsilon_{20}$, and $\varepsilon_{30}$ are the principal values of the dielectric tensor for the chiral tilted smectics at optical wavelengths, and $\theta$ is a tilt angle of the director with respect to the smectic layer normal.

The temperature dependencies of the ORP obtained at four fixed wavelengths of light can be transformed into the wavelength dependencies of the ORP at fixed temperatures. These dispersion dependencies of the ORP were fitted using

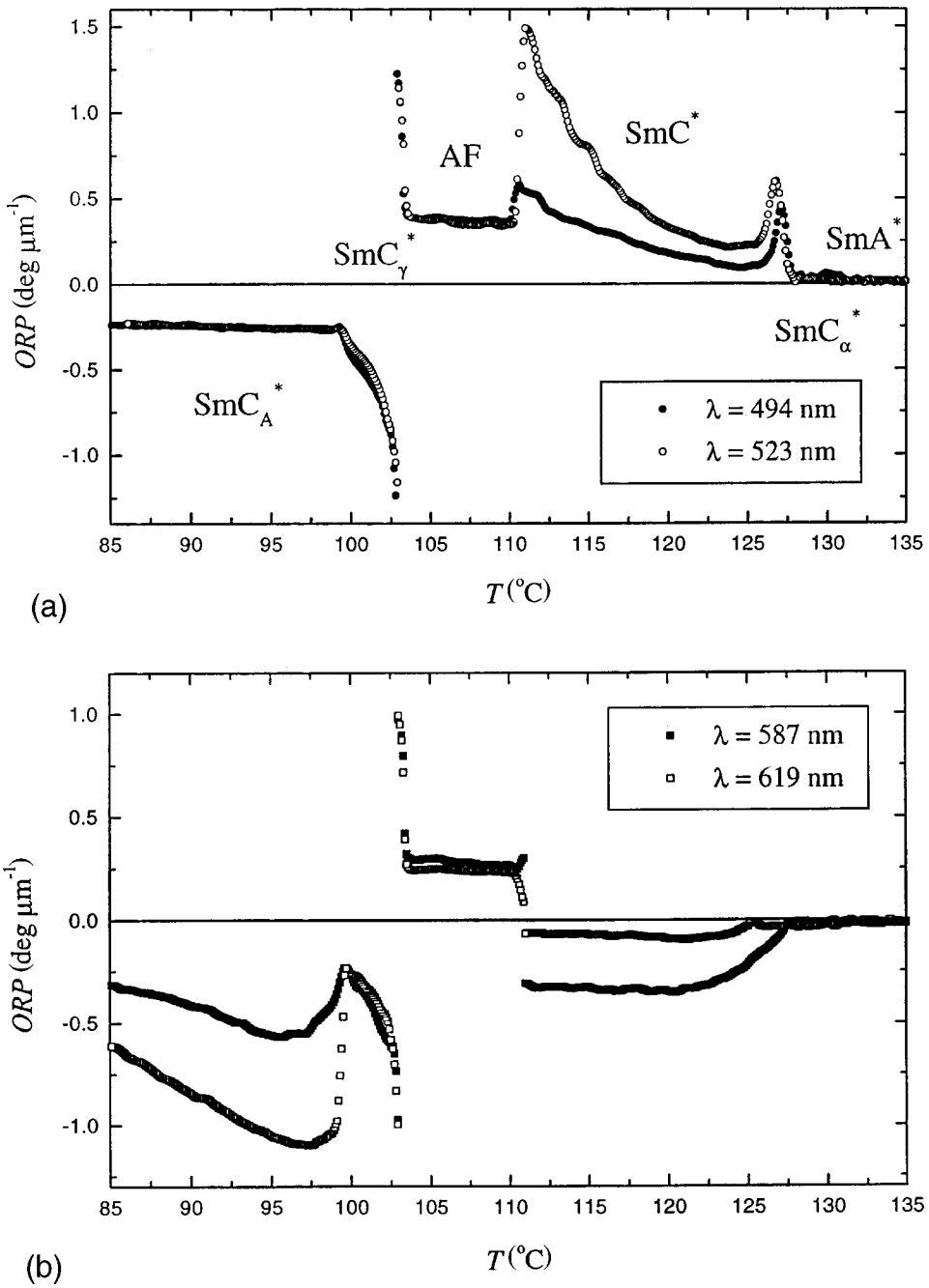


FIG. 4. Temperature dependencies of the ORP in the homeotropic cell of 11OTBBB1M7 during cooling. (a) For blue-green (494 nm) and green (523 nm) light. (b) For yellow (587 nm) and red (619 nm) light.

Eq. (2) to obtain the temperature dependence of the parameter $nP$, which is equal to the wavelength of selective reflection (SR) in several smectic phases. In this fitting procedure we neglect the dispersion of refractive indices, since its influence on the ORP dispersion is much smaller than that of the denominator $\lambda'^2(1-\lambda'^2)$. The fitting of ORP experimental data gave very reasonable values for the SR wavelength in Sm$C^*$, Sm$C^*_{FI2}$, and Sm$C^*_A$ phases (Fig. 5). In the Sm$C^*_{FI1}$ phase no reasonable results for the pitch could be obtained using the fitting procedure. This seems to be due either to the absence of a helical structure in the Sm$C^*_{FI1}$ phase or to the fact that the pitch is too large and the condition of pure optical rotation [13] $\lambda > P(n_e - n_o)$ is not fulfilled.

The observed colors of the selective reflected light for Sm$C^*$ and Sm$C^*_A$ phases allow for a check on the calculated SR wavelength values. The pitch value can easily be estimated from the SR wavelength by assuming that the mean refractive index $n$ is about 1.5, and that the wavelength of SR light is related to the full pitch in the Sm$C^*$ phase and to the half pitch in the Sm$C^*_A$ phase. In the high-temperature region of the Sm$C^*$ phase, the SR wavelength increases with decreasing temperature, up to 0.56 $\mu$m. At 122 °C the pitch is 0.37 $\mu$m. Then the SR wavelength decreases slowly until the

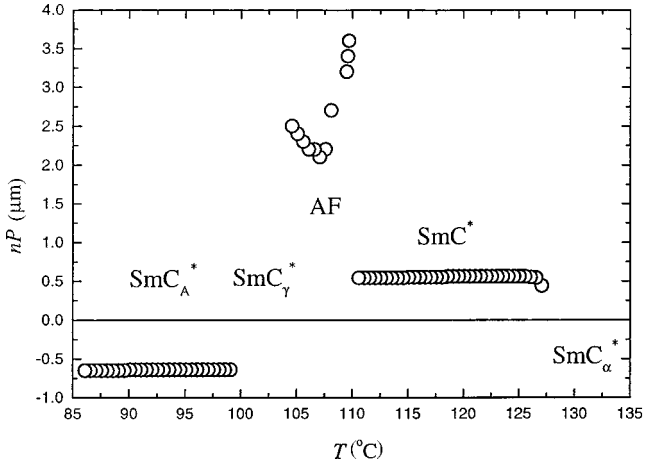


FIG. 5. Temperature dependence of the selective reflection wavelength $nP$ in several smectic phases of 11OTBBB1M7 obtained by fitting the ORP data using Eq. (2).

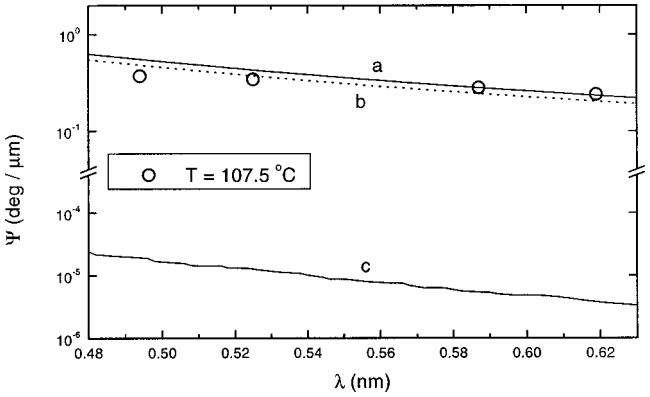


FIG. 6. Experimental data at a temperature of 107.5 °C and the simulated ORP spectra in Sm$C^*_{FI2}$ phase for the (a) modified Ising model (angles $\varphi_F = 3.7°$ and $\varphi_A = 1.6°$), (b) the distorted clock model (the angle of distortion $\delta = 69°$) (in terms of Johnson *et al.* [18], this angle is 21°). (c) A clock model with a long pitch superimposed on it, with the angular deviation between neighboring layers taken to be 0.5°, from 90°.

phase transition to the Sm$C^*_{FI2}$ phase; the corresponding color of the selective reflected light is green. In the Sm$C^*_A$ phase the SR wavelength is about 0.65 $\mu$m, and demonstrates a slow increase when temperature decreases; the corresponding pitch is $-0.86$ $\mu$m. In the middle region of the Sm$C^*_{FI2}$ phase, the SR wavelength is about 2 $\mu$m, and the corresponding pitch is $P = 2.8\,\mu$m if the periodicity of the dielectric permittivities tensor in this phase is half the pitch of the Sm$C^*_A$ phase. In the Sm$C^*_A$ phase, the sense of the helix is left handed, opposite to what is observed for the Sm$C^*$ phase. This change of helix's handedness in the Sm$C^*_A$ phase with respect to that in the Sm$C^*$ phase is consistent with the results of liquid-crystal-induced circular dichroism measurements [15]. The reversal of the helix occurs during the phase transition from Sm$C^*_{FI2}$ to Sm$C^*_{FI1}$ phases. This fact allows the two phases to be distinguished.

There were several models proposed for describing the molecular arrangements in Sm$C^*_{FI1}$ and Sm$C^*_{FI2}$ phases. All of these models are based on unit cells consisting of three and four smectic layers, and differ only in the details of the azimuthal angle progressions in unit cells. The simple Ising model [1,6] for the Sm$C^*_{FI2}$ phase is described by a sequence of azimuthal angles $\varphi_j$, having only two values 0 and $\pi$. For this model the four-layer sequence of azimuthal angles is $(0,0,\pi,\pi)$. The macroscopic chirality of the structure with a long helical pitch $P$ makes the sequence of azimuthal angles follow $(0,\varphi_{FI},\pi+2\varphi_{FI},\pi+3\varphi_{FI})$, where $\varphi_{FI}=2\pi h/P$ is the rotation angle between adjacent layers, and $h$ is the thickness of smectic layer. This azimuthal distribution of the director in the smectic layers forming the unit cell leads to the high optical anisotropy of the unit cell in a plane parallel to the smectic layers. The simple Ising model explains well the results of optical studies of the Sm$C^*_{FI2}$ phase, but Mach and co-workers [3,4] found that it cannot account for the both quarter- and half-order resonant peaks of x-ray-diffraction experiments. Recently, a modified Ising model was proposed [14], which does not contradict the resonant x-ray experiments. The modified Ising model is described by a sequence of azimuthal angles in a four-layer unit cell $(-\varphi_A, -\varphi_A+\varphi_F, \pi-2\varphi_A+\varphi_F, \pi-2\varphi_A+2\varphi_F)$, where $\varphi_A$ and $\varphi_F$ are the rotation angles of the **C** director between adjacent layers in the Sm$C^*_A$ and Sm$C^*$ phases, respectively. Since the difference in values of $\varphi_A$ and $\varphi_F$ is very small, the helical structures described by the simple and modified Ising models differ very slightly from each other.

The simple clock model [11] specifies a helical progression of azimuthal angle $\varphi_j$ from layer to layer with a fixed increment of $\Delta\varphi=\pi/2$ for a superlattice of the Sm$C^*_{FI2}$ phase. This helical four-layer periodical structure has a very small ORP of the order of $P^3_{SP}/\lambda^4$ when a short pitch $P_{SP}$ is approximately 12–16 nm and the wavelength $\lambda$ of light is about 500 nm. In addition, the long pitch ($P$) chirality of the unit cell's azimuthal angle distribution causes an increment in the angle between adjacent layers of $\Delta\varphi=\pi/2+\varphi_{FI}$ and the sequence of azimuthal angles in the unit cell $(0,\ \pi/2+\varphi_{FI},\ \pi+2\varphi_{FI},\ 3\pi/2+3\varphi_{FI})$. The obtained helical structure can be considered as a rotation of the unit cell as a whole around the smectic layer normal with a long pitch $P$. The long pitch chirality disturbs the initial $\mathbf{4_1}$ symmetry of the unit cell, and gives a small biaxiality in the scale of the unit cell, but this value is too small to explain the magnitude of the ORP experimentally observed in the Sm$C^*_{FI2}$ phase. This is confirmed by the calculation of the ORP [Fig. 6(c)] in the Sm$C^*_{FI2}$ phase using a $4\times4$ matrix method [16]. The parameters used in this calculation were as follows: the sample thickness $d=15\,\mu$m; the layer spacing $h=3.8$ nm [3]; the indices of refraction $n_3=1.639$ along the director, $n_2=1.497$ perpendicular to the tilt plane, and $n_1=1.495$ along the third principal axis; the tilt angle of the director $\theta=27.5°$ [10]; and the pitch of the helix structure $P=2.8\,\mu$m.

The distorted clock model with a symmetric sequence of azimuthal angles $\varphi_j=(\pi/2)j-\delta/2+(-1)^j\delta/2$, where $0\leqslant j\leqslant3$, was proposed [17] for the Sm$C^*_{FI2}$ phase to make the clock model consistent with the optical data. The sequence of azimuthal angles in this model is $(0,\ \pi/2-\delta,\ \pi,3\pi/2$

$-\delta$). This structure has a $\mathbf{2_1}$ symmetry and biaxial optical properties. The simple Ising model is a particular case of the distorted clock model with $\delta=\pi/2$. If a long pitch chirality is added, then the azimuthal angles progression becomes $(0, \pi/2-\delta+\varphi_{FI}, \pi+2\varphi_{FI}, 3\pi/2-\delta+3\varphi_{FI})$. This model, called the ''highly biaxial model,'' was used for describing the ellipsometric data obtained in the Sm$C^*_{FI1}$ and Sm$C^*_{FI2}$ phases of freestanding films [18]. It was shown that this structure is also able to explain the resonant x-ray-diffraction results. The simulation of the ORP in this case is presented in Fig. 6(b) for the distortion parameter $\delta=69°$. This angle corresponds to a distortion angle of $\pi/2-\delta$, in terms of Johnson *et al.*'s definition [18]. This value is not too far from the angle of 10° found by Johnson *et al.* for a different compound. This shows that the director distribution though the following clockwise distribution makes the structure of the AF (Sm$C^*_{FI2}$) phase more Ising-like.

The results of the ORP simulations presented in Fig. 6 show that both the modified Ising model [14] and the highly distorted clock model [17,18], specifying highly biaxial helical structures, can account for the values of the ORP in the Sm$C^*_{FI2}$ phase. The various angles used in the simulations are given in the figure caption. These models can also explain the fine structure of the peaks of the resonant x-ray diffraction observed in Sm$C^*_{FI1}$ and Sm$C^*_{FI2}$ phases [3,4]. To determine which of these two models is valid, it is necessary to make more accurate experimental investigations of the structural and optical properties of Sm$C^*_{FI1}$ and Sm$C^*_{FI2}$ phases in different AFLC compounds.

## IV. CONCLUSIONS

In thin samples of 11 OTBBB1M7 with homeotropic alignment, the phases Sm$C^*_A$, Sm$C^*_{FI1}$, Sm$C^*_{FI2}$, Sm$C^*$, Sm$C^*_\alpha$, and Sm$A^*$ were distinguished from each other. The sequence of the phases and their transition temperatures correspond to those observed in a bulk sample [10].

It was found that the optical rotatory power (ORP) demonstrates a characteristic change at the phase transitions. The sense of the helix in the Sm$C^*_A$ phase is found to be opposite to that in the Sm$C^*$ phase. This finding is consistent with the results from liquid-crystal-induced circular dichroism measurements [15]. The inversion of the helix's handedness, occurring during the phase transition from Sm$C^*_{FI2}$ to Sm$C^*_{FI1}$ phases, allows these phases to be identified using these techniques.

The pitches in the Sm$C^*_A$, Sm$C^*_{FI2}$, and Sm$C^*$ phases have been found using a fitting procedure of the ORP spectra for different temperatures. The results of the ORP simulations, using a $4\times4$ matrix method for Sm$C^*_{FI2}$ phase, show that only highly biaxial models, such as the modified Ising model [14] or the distorted clock model [17,18] can explain the experimental values of the ORP in the Sm$C^*_{FI2}$ phase. The clock model with a long pitch superimposed onto it gives rise to a very low value of the ORP, and this cannot explain the experimental results.

## ACKNOWLEDGMENTS

This work was supported by Enterprise Ireland and partly by the European ORCHIS network. We thank Dr. M. I. Barnik for supplying us with the aligning agent chromolane purchased from AURAT joint Co., 4 Likhachevski per. d. 6, 125438 Moscow, Russia. Trinity Trust of Trinity College, Dublin is thanked for funding the costs of color reproduction in this paper.

[1] A. Fukuda, Y. Takanishi, T. Isozaki, K. Ishikawa, and H. Takezoe, J. Mater. Chem. **4**, 997 (1994).
[2] N. M. Shtykov, J. K. Vij, R. A. Lewis, M. Hird, and J. W. Goodby, Phys. Rev. E **62**, 2279 (2000).
[3] P. Mach, R. Pindak, A.-M. Levelut, P. Barois, H. T. Nguyen, C. C. Huang, and L. Furenlid, Phys. Rev. Lett. **81**, 1015 (1998).
[4] P. Mach, R. Pindak, A.-M. Levelut, P. Barois, H. T. Nguyen, H. Baltes, M. Hird, K. Toyne, A. Seed, J. W. Goodby, C. C. Huang, and L. Furenlid, Phys. Rev. E **60**, 6793 (1998).
[5] B. Žekš and M. Cepič, Liq. Cryst. **14**, 445 (1993).
[6] T. Isozaki, K. Hiraoka, Y. Takanishi, H. Takezoe, A. Fukuda, Y. Suzuki, and I. Kawamura, Liq. Cryst. **12**, 59 (1992).
[7] P. Bak and R. Bruinsma, Phys. Rev. Lett. **49**, 249 (1982).
[8] M. Yamashita and S. Tanaka, Jpn. J. Appl. Phys. **37**, L528 (1998).
[9] S. Pikin, M. Gorkunov, D. Kilian, and W. Haase, Liq. Cryst. **26**, 1107 (1999).
[10] H. T. Nguyen, J. C. Rouillon, P. Cluzeau, G. Sigaud, C. Destrade, and N. Isaert, Liq. Cryst. **17**, 571 (1994).
[11] M. Cepič and B. Žekš, Mol. Cryst. Liq. Cryst. **263**, 61 (1995).
[12] D. Schlauf, Ch. Bahr, and H. T. Nguyen, Phys. Rev. E **60**, 6816 (1999).
[13] P. G. de Gennes and J. Prost, *The Physics of Liquid Crystals* (Clarendon, Oxford, 1993), p. 277.
[14] T. Akizuki, K. Miyachi, Y. Takanishi, K. Ishikawa, H. Takezoe, and A. Fukuda, Jpn. J. Appl. Phys. **38**, 4832 (1999).
[15] K. Yamada, Y. Takanishi, K. Ishikawa, H. Takezoe, A. Fukuda, and M. A. Osipov, Phys. Rev. E **56**, R43 (1997).
[16] D. W. Berreman, J. Opt. Soc. Am. **62**, 502 (1972).
[17] A.-M. Levelut and B. Pansu, Phys. Rev. E **60**, 6803 (1999).
[18] P. M. Johnson, D. A. Olson, S. Pankratz, H. T. Nguyen, J. W. Goodby, M. Hird, and C. C. Huang, Phys. Rev. Lett. **84**, 4870 (2000).